Methanol and Ethanol Electro-oxidation on to Platinum Loaded Reduced Graphene Oxide Surface for Fuel Cell Application

Debalina Das[1], I. Basumallick[1*] and Susanta Ghosh[2*]

[1]*Department of Chemistry, Electro-Chemistry Laboratory, Visva-Bharati University, Santiniketan-731235, India.*
[2]*Integrated Science and Research, Visva-Bharati University, Santiniketan-731235, India.*

Authors' contributions

This work was carried out in collaboration between all authors. All authors read and approved the final manuscript.

Article Information

Original Research Article

ABSTRACT

We report here electro-oxidation of methanol (MeOH) and ethanol (EtOH) onto Platinum (Pt) loaded reduced graphene oxide/Carbon-felt surface (Pt/rGO/C-felt). Graphene oxide was prepared by Hummer's method using exfoliation technique. Apparent activation energies of electro-oxidation of methanol (MeOH) and ethanol (EtOH) onto Pt/rGO/C-felt and Pt/C-felt surfaces were determined from cyclic-voltammetry studies at different temperatures. It was observed that apparent activation energies of MeOH and EtOH oxidation onto Pt/rGO/C-felt surfaces have been reduced compared to those of Pt/C-felt surface. This indicates rGO surface plays a key role in enhancing electro-oxidation process providing efficient adsorption and de-protonation sites.

Keywords: Reduced graphene oxide; platinum; methanol and ethanol oxidation; activation energy.

1. INTRODUCTION

In continuation of our earlier studies on electro oxidation of Ethanol and Ethylene glycol on to nano Pt and PtRu loaded carbon felt electrode [1], we report here similar studies on to Pt loaded reduced graphene Oxide (rGO) surface. Methanol (MeOH) [2,3] and Ethanol (EtOH) [4,5]

Corresponding author: E-mail: ibasumallick@yahoo.co.uk, susanta.ghosh@visva-bharati.ac.in;

are most attractive fuels for direct alcohol fuel cells (DAFCs) , because of low-toxicity and less volatile nature of these alcohols. However, major problems arise such as high cost of noble metals, slow reaction kinetics, poor selectivity and catalyst poisoning by CO [6,7] make this process unattractive for large scale application [8]. The transition-metal-based catalysts (Pt, Ru, Mo, Sn etc.) are often susceptible to poisoning because of their metal carbonyl forming propensity.

The activity of the catalyst and their better utilisation often depend upon the role of support material used. The support materials should have high specific surface area, good electronic conductivity and anti-corrosion property [9]. The commonly used catalyst supports are carbon black, nano fibres, carbon nano tubes, meso-porous carbon, carbon-felt etc [10-12]. However, the main problem of using C-felt as catalyst support material is that its surface is highly hydrophobic and often need functionalization [13] for improving hydrophilic character.

In recent years, Graphene oxide (GO) and partially reduced Graphene Oxide (rGO) are drawing attention as new generation of catalyst support due to their high specific surface area, with unique graphitized basal plane structure having excellent electrical, mechanical and thermal properties [14,15]. In spite of several studies on synthesis of graphene/rGO and their applications in different catalytic reactions, electro-catalytic activities of rGO supported Pt nanoparticles or nano Pt dendrites [16,17] towards alcohol oxidation are limited. Previously, rGO/Pt composite was prepared by co-reduction of graphene oxide and metal precursor salt by chemical method using $NaBH_4$, hydrazine hydrate, ethylene glycol, 1, 2-propanediol etc. as reducing agents [16,18-20]. Sharma et al. [21] synthesized reduced graphene oxide/platinum supported electro catalysts by employing a fast and eco-friendly microwave-assisted polyol process and employed as an anode material for the electro-oxidation of methanol. Qiu et al. [2] successfully synthesised platinum nanoparticles (Pt NPs) with uniform size and high dispersion on poly (diallyl dimethyl ammonium chloride) functionalized graphene oxide via a sodium boro-hydride reduction process. They showed a good electro catalytic activity toward methanol oxidation and oxygen reduction. Chen et al. [22] have reported a nontoxic, rapid, one-pot and template-free synthesis of three-dimensional

(3D) Pt nano flowers (PtNFs) supported on graphene oxide (GO) nano sheets by using ethanol as a reductant. Divya et al. [23] prepared platinum nanoparticles on graphene sheets by ascorbic acid reduction and employed as electro catalysts for both oxygen reduction reaction and hydrogen oxidation reaction in proton exchange membrane fuel cells. However, such preparation method involved tedious purification of the composite [24].

Electrochemical reduction of graphene oxide to rGO is a greener way of obtaining rGO and electro deposition of Pt onto rGO. This process is hazardless, effective and controllable method. Shao et al. [25] synthesised electro-chemically reduced graphene oxide (ER-G). The oxygen content was significantly decreased in ER-G and the sp^2 carbon was restored after electrochemical reduction which exhibited much higher electrochemical capacitance and cycling durability than carbon nanotubes (CNTs) and chemically reduced graphene. Chen et al. [26] reported a direct deposition of graphene nano sheet onto a glassy carbon electrode through cyclic voltammetric reduction from a graphene oxide colloidal solution.

The electro oxidation of Ethanol and Ethylene glycol on to nano Pt and Pt/Ru loaded carbon felt electrode were reported from our laboratory [1]. We observed that the apparent activation energies for oxidation of EtOH and EG pass through a minimum at about 15–20 at. % of Ru in the PtRu alloy catalysts. Eda et al. [27] and Zhu et al. [14] reported that graphene or rGO will provide a large surface area for dispersion of Pt catalyst and this composite enhances methanol electro- oxidation rate. Wang et al. [3] reported electro-oxidation of methanol onto Pt loaded rGO, prepare by pulse electro-deposition technique and observed enhancement of oxidation rate. Very recently methanol and ethanol electro-oxidation onto Pt-Ru loaded 3D graphene foam has been reported by Liu et al. [27b] and these authors observed both enhancement of catalytic activity and CO tolerance.

The present study is focused on the study of kinetics of electro-oxidation of MeOH and EtOH on to Pt/rGO/C-felt and Pt/C-felt surfaces for determination of activation energies of these electro-oxidation reactions in order to understand the role of rGO in the electro-oxidation process.

2. EXPERIMENTAL

2.1 Materials and Methods

Graphite and H_2PtCl_6 were obtained from Alfa-Aeser (India). All other chemicals such as $KMnO_4$, $NaNO_3$, H_2SO_4, HCl, and 30% H_2O_2 were obtained from Merck (India).

2.2 Preparation of Graphite Oxide and Graphene Oxide (GO)

2.2.1 Preparation of graphite oxide

Graphite oxide was prepared in the laboratory by following Hummer's Method [28]. 3 g of Graphite flakes were mixed with 1.5 g $NaNO_3$ and 69 ml of concentrate sulphuric acid in a beaker and stirred vigorously. The mixture was then kept at 0ºC in an ice bath for 5 minutes. In the next step, 9 g $KMnO_4$ was added slowly with small amount at a time under constant stirring keeping the bath temperature below 20ºC during addition. The temperature of the reaction bath was raised to 30-35ºC and kept at this temperature for 30 minutes. The mixture gradually became pasty with evaluation of small amount of gas. 20 ml of water was added to the paste and the temperature of the solution was further increased to 98ºC and stirred constantly for another 15 minutes. 40 ml of water and 3 ml of 30% H_2O_2 were further added to ensure reduction of residual permanganate and MnO_2 to colourless soluble manganese sulphate. The suspension was filtered; residue was collected and washed thoroughly with de-ionised water (DI) water, 3% HCl and EtOH, simultaneously. After washing, the residue (graphite oxide) was dried in a hot air oven at 40ºC overnight.

2.2.2 Preparation of graphene oxide (GO)

Graphene oxide was prepared by suspending 0.025 g graphite oxide in 50 ml DI water and ultrasonicated for 1 hour for exfoliation. The homogeneous mixture was centrifuged at 3000 rpm for 30 minutes to get non-sediment supernatant solution [30]. After decanting the supernatant solution, the residue was washed, dried and characterized by Fourier transform infrared (FTIR) spectroscopy using Shimadzu FT-IR 8400 S (Fig. 2a).

2.3 Preparation of rGO from GO

GO ink was sprayed by using sprayer over carbon felt (C-felt) surface (1 cm length × 1 cm width, ca. 2.4 mm thickness, 0.95 porosity, mean fibre diameter of ca. 20 µm, electrical conductivity 10 S/m) and the C-felt was vacuum dried overnight. The loading of GO over C-felt electrode was approximately 1%. GO over the C-felt surface was reduced to rGO electrochemically in a bath containing 0.5 M H_2SO_4 solution, by passing a current of 1 mA/cm^2 for 30 minutes (Fig. 1a), and washed thoroughly by DI water. Fourier transform infrared (FTIR) spectroscopy of rGO was carried out using Shimadzu FT-IR 8400S (Fig. 2b).

2.4 Preparation of Working Electrode for Electrochemical Studies

Pt was deposited electro-chemically onto rGO/C-felt and bare C-felt surfaces, galvanostatically by passing a current of 2 mA/cm^2 for 900 seconds (Fig. 1b). Both electrodes were kept in two separate baths in series, each of which contains plating electrolyte of 3 mM H_2PtCl_6 in 0.5 M H_2SO_4. Those Pt loaded C-felt and rGO/C-felt electrodes was washed thoroughly with de-ionized water and used as working electrodes for MeOH and EtOH oxidation reaction. Considering smooth (noise free) Pt deposition curve (Fig. 1b), the Pt loading over C-felt surfaces was calculated assuming 100% faradic deposition. Pt deposition onto rGO surface was further confirmed from EDX analysis (Fig. 3d)

In fact C-felt has a micro-porous structure, it easily adsorbs colloidal GO particles by physisorption mechanism, the latter upon electro-reduction forms more conducting rGO-Cfelt surface. Electro-deposited Pt binds to this surface by atom to atom binding mode similar to its electro-deposition onto graphite surface. On the other hand Pt electro-deposited onto C-felt surface are less rigidly bound.

The electro-catalytic activities of Pt/rGO/C-felt and Pt/C-felt electrodes toward electro-oxidation of methanol and ethanol were examined using 1M MeOH and 1M EtOH in 0.5 M H_2SO_4 solution. The apparent activation energies for methanol and ethanol oxidation reaction were calculated from the CVs measured at different temperatures (288 – 318 K).

3. CHARACTERIZATION

Fourier Transform Infra-red Spectroscopy (FT-IR) graphs of GO and rGO were taken using Shimadzu FT-IR 8400S (Fig. 2). The surface

morphology of the electrodes was recorded by transmission electron microscope (TEM) (FEI TECNAI 200 KV) (Fig. 3.) and scanning electron microscope (SEM) (Hitachi S-3000N) (Fig. 3). For TEM analysis, Pt/rGO/C-felt electrode was dispersed in ethanol and ultrasonicated for 10 minutes. A few drops of the suspension was deposited onto TEM grid and evacuated before analysis.

Electrochemical measurements were carried out using a three electrode cell configuration by a potentiostat–galovanostat (PAR, VersaStat^{TM} II). A Pt-foil was used (1 cm^2) as a counter electrode and a saturated calomel electrode as reference electrode. The electrolytic solutions taken in the cell were 1 M MeOH or 1 M EtOH in 0.5 M H_2SO_4. Cyclic voltammetry experiments were carried out at five different scan rates, 10, 30, 50, 70 and 90 mV/s and at four different temperatures, 288, 298, 308, and 318 K.

4. RESULTS AND DISCUSSION

4.1 Electrochemical Reduction of GO to rGO and Pt Electro-deposition

GO onto C-felt was reduced to rGO galvanostatically in a bath containing 0.5 M H_2SO_4 solution, by passing a current of 1 mA/cm^2 for 30 minutes (Fig. 1a). The reduction of GO to partially reduced GO can be seen from the potential vs. time graph (Fig. 1a). Pt was electro-deposited onto rGO/C-felt surface and bare C-felt surface, galvanostatically by passing a current of 2 mA/ cm^2 for 900 seconds (Fig. 1b). Pt deposition onto rGO/C-felt has taken place at lower potential compared to bare C-felt surface and this is due to higher interfacial resistance at bare C-felt surface.

4.2 FT-IR Spectra of GO and rGO

FT-IR spectra of graphene oxide (GO) and reduced graphene oxide (rGO) are shown in Fig. 2a and Fig. 2b, respectively. The appearance of peaks at 3600-3400 cm^{-1} (-OH stretching vibrations), 1753 cm^{-1} (C=O stretching vibration), 1581 cm^{-1} (skeletal vibration from un-oxidized graphitic domains), 1421 cm^{-1} (aromatic C=C

stretching), 1226 cm^{-1} (C-OH stretching vibrations), 839 cm^{-1} (epoxy) indicates the formation of graphene oxide (Fig. 2a). Comparison between the FT-IR spectra of graphene oxide (Fig. 2a) and reduced graphene oxide (Fig. 2b) clearly shows that the –OH stretching vibrations of GO at 3600-3400 cm^{-1} are suppressed and -C=O stretching vibration at 1753 cm^{-1} is almost disappeared. However the appearance of the C=C stretching vibrations at 1620 -1680 cm^{-1} observed in FT-IR spectra of rGO (Fig. 2b) indicates the partial recovery of sp^2 graphitic network. The peaks obtained at 1050-1150 cm^{-1} might be due to the C-O stretching vibration of the hydroxyl moiety. From the FT-IR study, it is cleared that graphene oxide (GO) was partially reduced to rGO by the electrochemical method. The formation of rGO from GO can be further evidenced from our earlier study [**Error! eference source not found.**] and also from the studies of Choi et al. [30] and Dreyer et al. [31].

4.3 HR-TEM, SEM Images and EDX Spectra

The HR-TEM image of electro-deposited Pt nano particles onto rGO surface is shown in Fig. 3a. TEM images clearly show that the formation of agglomerated particles, which are spherical in shape, but size varied from 40-50 nm.

SEM images of Pt nano particles decorated onto rGO/C-felt support are illustrated in Fig. 3b. From the image it is cleared that the Pt nano particles were uniformly distributed onto rGO/C-felt surface and they took almost spherical shape within 40-50 nm range. The SEM image of exfoliated rGO onto C-felt was shown in Fig. 3c. The energy dispersive X-Ray pattern (EDX) of Pt/rGO composite is shown in Fig. 3d. The EDX spectrum shows the peaks corresponding to C, O, and Pt elements, which confirmed the deposition of Pt nano particles onto rGO nano sheets. From the spectrum it can be further demonstrated that peaks at 0.3 keV, 0.5 keV and 2.1 keV respectively indicated the C (79 atom %), O (20.24 atom %) and Pt (0.025 atom %). There is a combined peak of C and Pt at 0.3 keV indicated Pt deposition on to reduced graphene oxide surface. This can be further evidenced from the works of He et al. [32].
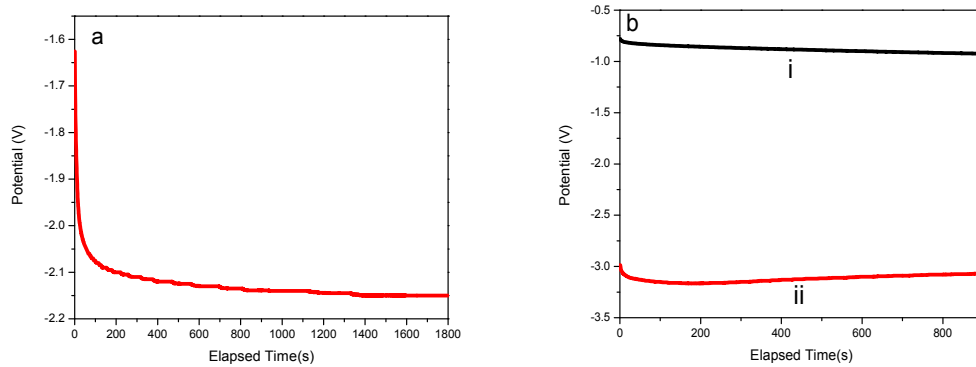
Fig. 1. a) Galvenostatic reduction of GO in 0.5 M H$_2$S0$_4$ at 1 mA/ cm^2. b) Galvenostatic deposition of Pt from chloro platinic acid at 2 mA/ cm^2 onto i) rGO/C-felt ii) rGO/C-felt and C-felt in series
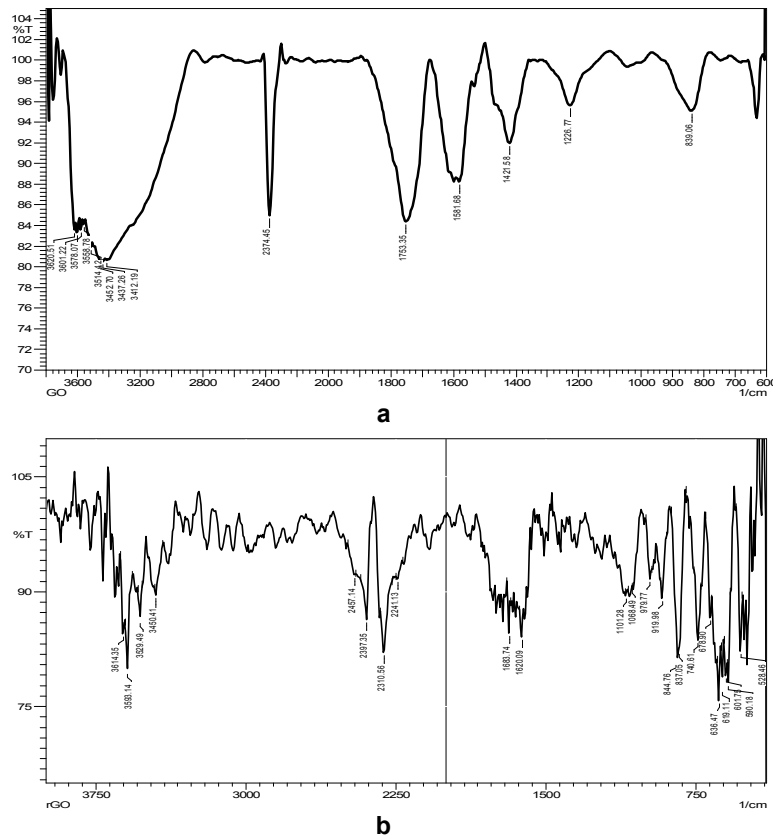

Fig. 2. FT-IR spectra of a) Graphene Oxide (GO) b) Reduced Graphene Oxide (rGO)

4.4 Electrochemical Studies

4.4.1 Determination of effective surface area (EAS) of working electrodes

Effective surface area (EAS) of the working electrodes (Pt/rGO/C-felt and Pt/C-felt) was determined by under potential deposition of copper (Cu-UPD) [33]. EAS of these electrodes were 109.4 cm^2/ mg for Pt/rGO/C-felt and 65 cm^2/ mg for Pt/C-felt. It was observed that the surface area of Pt onto rGO was enhanced up to 40.6% compared to that of Pt deposited onto C-felt surface under identical condition.

4.4.2 Cyclic-voltammetry studies

CVs of 1 M MeOH and 1 M EtOH in 0.5 M H_2SO_4 onto Pt/rGO/C-felt and Pt/C-felt electrodes at a scan rate of 50 mV/s at 308 K are shown in Fig. 4a and Fig. 4b, respectively. It is seen that both MeOH and EtOH showed similar anodic peaks in the forward scan and reverse scan. The peak appeared in reverse scan are due to oxidation of CO or residual carbonaceous species present on the electrode surface. Comparing the CV diagrams of MeOH and EtOH onto Pt/rGO/C-felt and Pt-C-felt surface, it is found that the forward peak current densities are enhanced by 5 times for MeOH and 1.5 times for EtOH (Table 1). Thus, enhancement of anodic peak currents on to Pt/rGO/C-felt electrode primarily indicates better catalytic behaviour. The forward peak

current to back peak current (I_F / I_B) ratios for MeOH are 1.4 (Pt/rGO/C-felt) and 1.35 (Pt/C-felt) and for EtOH 2.2 (Pt/rGO/C-felt) and 1.77 (Pt/C-felt) (Table 1). This indicates that for EtOH oxidation the Pt/rGO/C-felt electrode shows better tolerance towards CO poisoning.

Table 1. Peak currents (I_F and I_B) values of MeOH and EtOH electro oxidation onto Pt/rGO/C-felt and Pt/C-felt surfaces from CV study at scan rate 50 mV/ s at 308 K

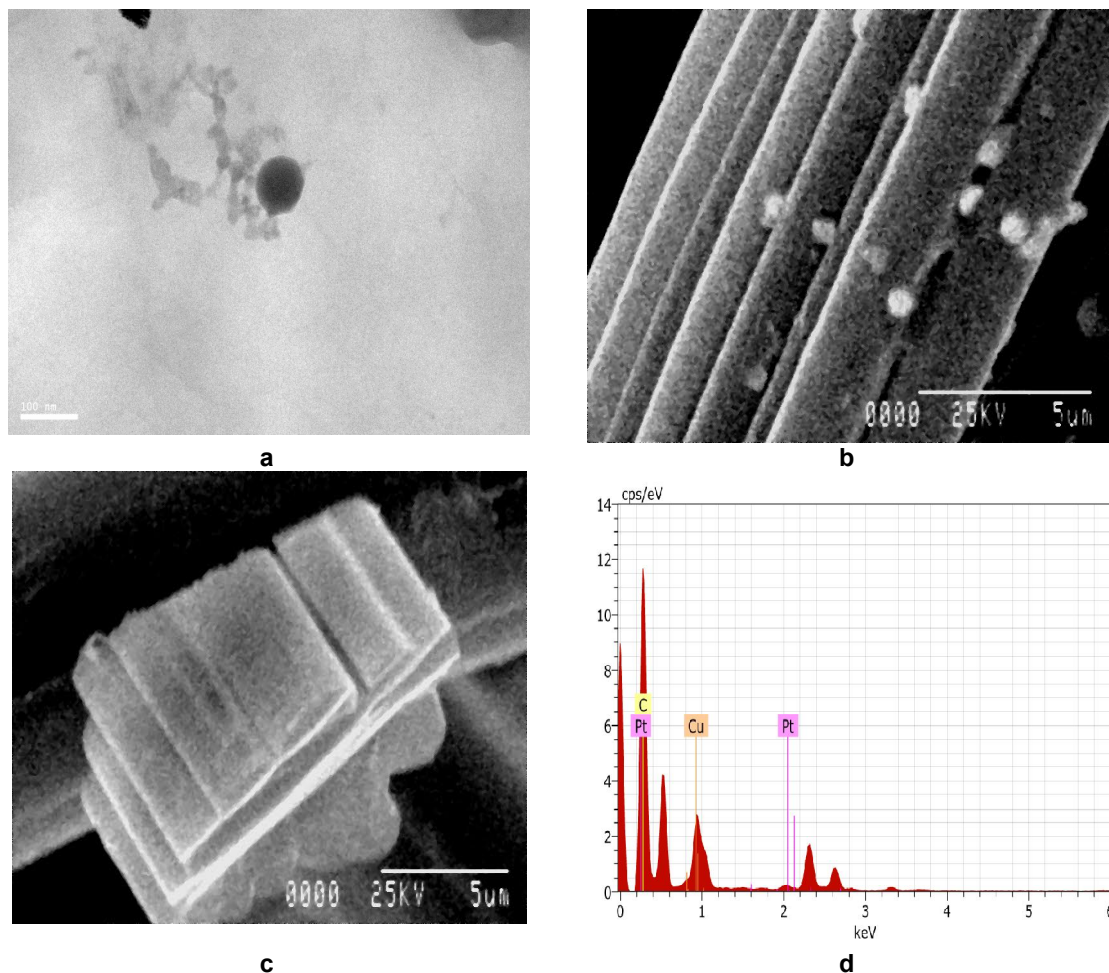|	Pt/r GO/C-felt			Pt/C-felt		
	I_F	I_B	I_F / I_B	I_F	I_B	I_F / I_B
MeOH	31.2	22.8	1.4	6.1	4.5	1.35
EtOH	9.9	4.6	2.2	6.3	3.55	1.77

Fig. 3. TEM image of a) Pt nano particles onto rGO surface b) SEM image of Pt nano particles onto rGO/C-felt surface c) SEM image of exfoliated rGO onto C-felt surface d) EDX spectra of Pt/rGO composite
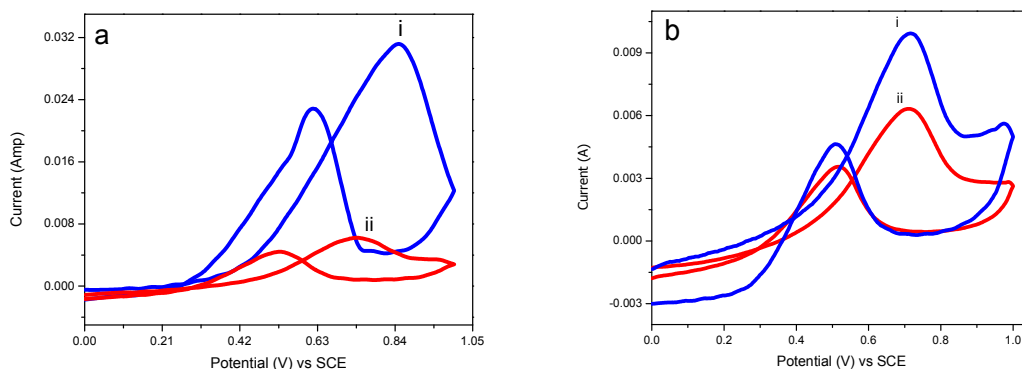
Fig. 4. Cyclic voltammograms of 1 M Methanol and 1 M ethanol in 0.5 M H$_2$SO$_4$ at scan rate 50 mV/ s at 308 K, (a) Methanol and (b) Ethanol oxidation onto (i) Pt/rGO/C-felt (ii) Pt/C-felt

4.4.3 Determination of the apparent Activation Energy for MeOH and EtOH oxidation

Arrhenius plots for electro-oxidations of MeOH and EtOH were drawn by calculating apparent rate constant (k) values using the equation (1) [40], where n = no of electrons involved in the oxidation process (n = 6 for MeOH, n = 12 for EtOH, assuming complete oxidation), F = Faraday constant, i = average current density over all scan rate at the selected potentials.

$$i = n F k \qquad (1)$$

The forward anodic current values for the electro-oxidation of MeOH and EtOH onto Pt/rGO/C-felt and Pt/C-felt were taken at a fixed potential of 0.7 V under the temperature range of 288–318 K. All the current values are normalized with respect to effective surface area (EAS) and the catalyst loading factor is expressed as i / cm^2.mg.

Typical Arrhenius plots for MeOH and EtOH were obtained by plotting log k (k/ mol cm^{-2} s^{-1} mg^{-1}) vs. 1/T (Fig. 5.). Average linear plots were drawn using the linear fit application of Origin 8.5 software (UK). From the slopes of the curves, the apparent activation energy for the electro-oxidation of MeOH and EtOH were calculated and presented in Table 2. From Table 2, it is cleared that activation energies for electro oxidation of MeOH onto Pt/rGO/C-felt is lowered by 4 kJ/mol (at E = 0.7 V) as compared to Pt/C-felt electrode. Similarly, for EtOH oxidation activation energy values of Pt/rGO/C-felt are lowered by 7.5 kJ/mol (at E =0.7 V) in comparison with Pt/C-felt electrode. This is a

clear indication of a better catalytic activity on to Pt/rGO/C-felt electrode compared to Pt/C-felt electrode.

Table 2. Apparent activation energy values of MeOH and EtOH electro oxidation (E= 0.7 V) onto Pt/rGO/C-felt and Pt/C-felt surfaces

	Apparent energy of activation (E=0.7 V)	
	Pt/rGO/C-felt	**Pt/C-felt**
Methanol	32.5	36.4
Ethanol	18	25.5

4.4.4 Effect of scan rate

The kinetic studies of the MeOH and EtOH electro-oxidation on to Pt/rGO/C-felt and Pt/C-felt are recorded at different scan rates (10, 30, 50, 70 and 90 mV/s). The relationship between the forward peak current (I$_{pa}$) and $\sqrt{v}$ (Figs. 6a, 6b) and forward peak potential (E$_{pa}$) and log v (v = scan rate) (Fig. 6c, 6d) are taken for both MeOH and EtOH on to Pt/rGO/C-felt and Pt/C-felt electrodes. The linear relationship for the plot of I$_{pa}$ vs $\sqrt{v}$ indicated that electro-oxidation of MeOH and EtOH are controlled by the diffusion process. Further the linear correlation for the plot of E$_{pa}$ vs log v indicated that oxidation of MeOH and EtOH are irreversible process.

4.4.5 Amperometric study of EG on to Pt/C-felt and Pt/rGO/C-felt electrodes

Steady state amperometric study has been carried out for electro-oxidation of EtOH onto Pt/rGO/C-felt and Pt/C-felt electrodes at

potentials of 0.5 V (Fig. 7a) and 0.15 V (Fig. 7b), respectively. Those curves for EtOH oxidations clearly indicate better oxidation features onto Pt/rGO/C-felt surface compared to Pt/C-felt surface.
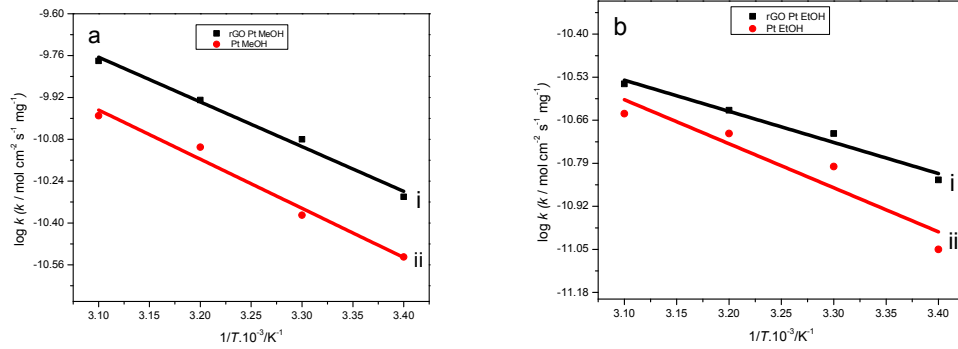

Fig. 5. Arrhenius plots for a) Methanol and b) Ethanol electro-oxidation onto i) Pt/rGO/C-felt and ii) Pt/C-felt catalyst at potential of 0.7 V
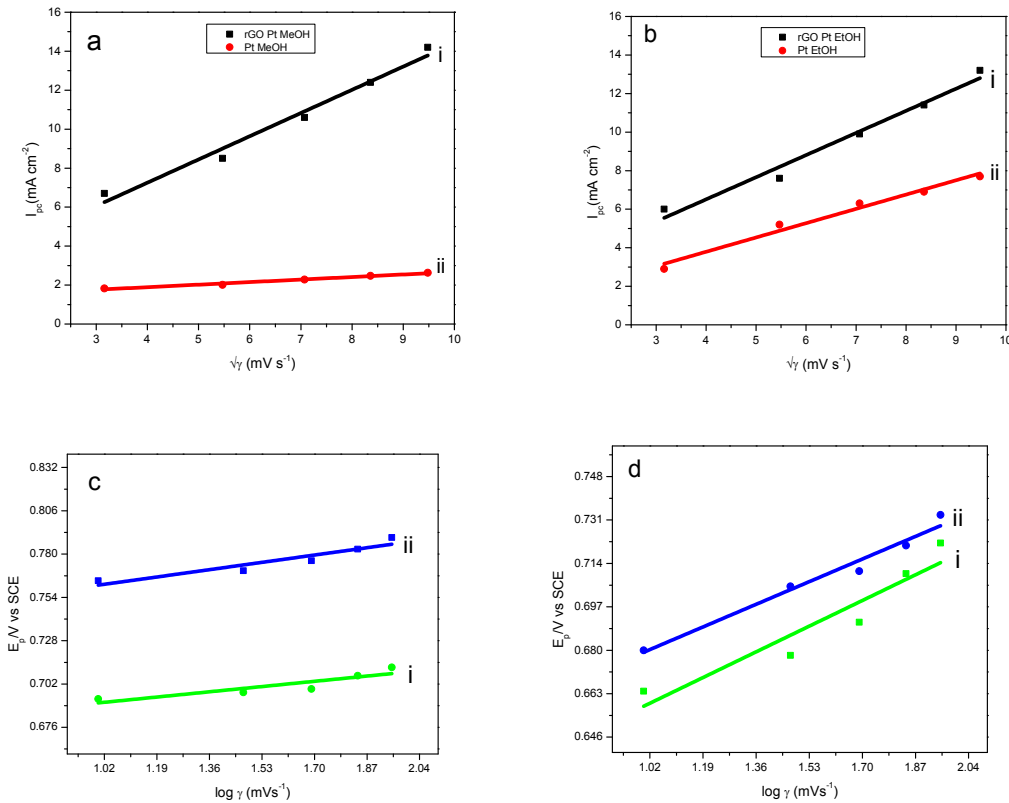

Fig. 6. (a) (b) I_{pc} vs $\sqrt{v}$ and (c) (d) E_{pc} vs log v plots of i) Pt/rGO/C-felt and ii) Pt/C-felt at different scan rates (10, 30, 50, 70 and 90 mV/s) for MeOH (a, c) and EtOH (b, d)
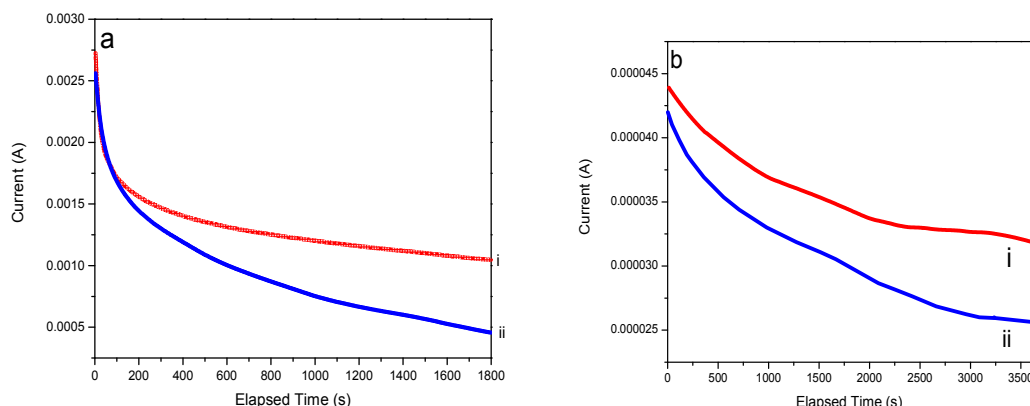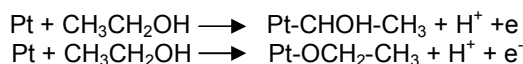
Fig. 7. Amperometric *i–t* curves of EtOH electro-oxidation onto i) Pt/rGO/C-felt and ii) Pt/C-felt catalysts in 1 M EtOH and 0.5 M H_2SO_4 at a) 0.5 V b) 0.15 V
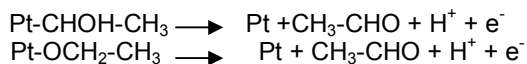
4.5 Proposed Model of Electro-oxidation

The enhanced electro-catalytic activity of MeOH and EtOH onto Pt/rGO/C-felt compared to Pt/C-felt can be explained by considering the primary steps [35] of electro-oxidation of EtOH which involve series of de-protonation and de-electronation reactions.

In general, the major reaction products of EtOH electro-oxidation are acetaldehyde [34,35] and acetic acid [35]. Primarily, EtOH adsorbs onto Pt either through C-adsorbing or O-adsorbing centre and subsequently de-protonates as shown below,

$$Pt + CH_3CH_2OH \longrightarrow Pt\text{-}CHOH\text{-}CH_3 + H^+ + e$$
$$Pt + CH_3CH_2OH \longrightarrow Pt\text{-}OCH_2\text{-}CH_3 + H^+ + e^-$$

It was shown that acetaldehyde is formed at low potential [41].

$$Pt\text{-}CHOH\text{-}CH_3 \longrightarrow Pt + CH_3\text{-}CHO + H^+ + e^-$$
$$Pt\text{-}OCH_2\text{-}CH_3 \longrightarrow Pt + CH_3\text{-}CHO + H^+ + e^-$$

When acetaldehyde is formed, it adsorbs on Pt and forms a $CH_3\text{-}CO\text{-}Pt$ species which undergoes further de-protonation and de-electronation.

$$Pt + CH_3\text{-}CHO \longrightarrow Pt\text{-}CO\text{-}CH_3 + H^+ + e^-$$

It was observed that C-C bond dissociation occurs at a potential of E< 0.4 V vs. saturated hydrogen electrode (SHE).

$$Pt\text{-}CO\text{-}CH_3 + Pt \longrightarrow Pt\text{-}CO + Pt\text{-}CH_3$$

At potential higher than 0.6 V vs. SHE the dissociation of adsorbed water can occur on Pt, forming the hydroxyl radicals, which assists oxidation of adsorbed CO to CO_2 as follows,

$$Pt\text{-}CO + Pt\text{-}OH \longrightarrow 2 Pt + CO_2 + H^+ + e^-$$

It is reported [1] that oxidation of Pt-CH_3 to CO_2 may occur at low potential with complete oxidation of EtOH.

It is expected that negatively charged surface of rGO (zeta potential is negative) will accelerate de-protonation steps of EtOH electro-oxidation. Admittedly, our current research is limited to predict the exact role of Pt/rGO composite in improving electro catalytic activity of (lowering the energy of activation) the catalyst towards MeOH and EtOH oxidation. Further research is essential to understand the mechanism behind the improved activity of Pt/rGO composite catalyst. However a qualitative model (Fig. 8.) indicating attachment of EtOH on to Pt/rGO surface followed by its H bond assisted deprotonation, similar to hydroxyl ion assisted deprotonation of ethanol on to nano gold surface [36] has been proposed assuming it is rate determining step of the multi- steps oxidation mechanism. It has been reported that electro-oxidation of methanol [3] onto these surfaces is also enhanced.
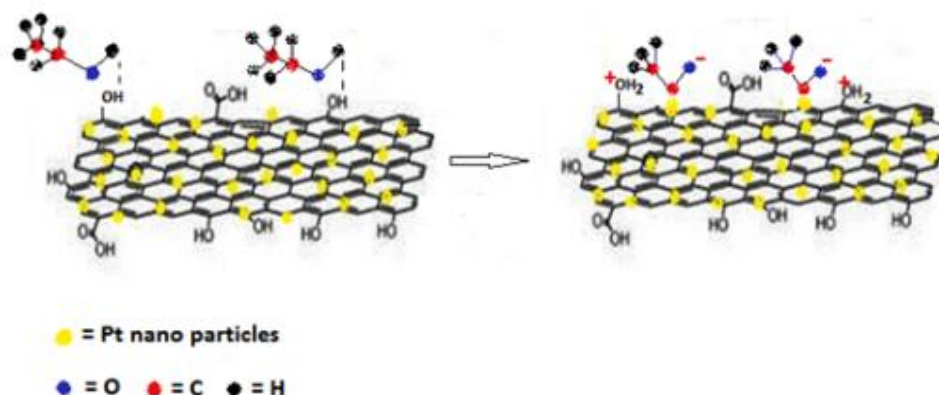
Fig. 8. Proposed model indicating attachment of EtOH on to Pt/rGO/C-felt surface followed by its H-bond assisted deprotonation

5. CONCLUSION

In the present study, we have shown that apparent activation energies of electro- oxidation of MeOH and EtOH onto electro-chemically synthesized Pt/rGO/C-felt electrodes are appreciably lowered than those onto Pt/ C felt. This has been explained on the basis of adsorption of MeOH and EtOH onto rGO-Pt composite surface. Similar calculations for the activation energies of CO oxidation (back peak) show that there is practically no change in activation energies for CO oxidation onto these surfaces.

COMPETING INTERESTS

Authors have declared that no competing interests exist.

REFERENCES

1. Chatterjee M, Chatterjee A, Ghosh S, Basumallick I. Electro-oxidation of ethanol and ethylene glycol on carbon-supported nano-Pt and -PtRu catalyst in acid solution. Electrochim. Acta. 2009;54:7299-7304.
2. Qiu JD, Wang GC, Liang RP, Xia XH, Yu HW. Controllable deposition of platinum nanoparticles on graphene as an electro catalyst for direct methanol fuel cells. J. Phys. Chem. C. 2011;115:15639-15645.
3. Ye W, Zhang X, Chen Y, Du Y, Zhou F, Wang C. Pulsed electro deposition of reduced graphene oxide on glass carbon electrode as an effective support of electro deposited Pt micro spherical particles: nucleation studies and the application for methanol electro-oxidation. Int. J. Electrochem. Sci. 2013;8:2122-2139.
4. Lai SCS, Kleyn SF, Rosca V, Koper MM. Mechanism of the dissociation and electro oxidation of ethanol and acetaldehyde on platinum as studied by SERS. J. Phys. Chem. C. 2008;112:19080-19087.
5. Liu Z, Ling XY, Su X, Lee JY, Gan LM. Preparation and characterization of Pt/C and Pt-Ru/C electro catalysts for direct ethanol fuel cells. J. of Power Sources. 2005;149:1-7.
6. Trens P, Durand R, Coq B, Coutanceau C, Rousseau S, Lamy C. Poisoning of Pt/C catalysts by CO and its consequences over the kinetics of hydrogen chemisorptions. Appl. Catal. B: Environ. 2009;92:280-284.
7. Canut JML, Abouatallah RM, Harrington DA. Detection of membrane drying, fuel cell flooding, and anode catalyst poisoning on PEMFC stacks by electrochemical impedance spectroscopy. J. Electrochem. Soc. 2006;153:857-864.
8. Ye W, Kou H, Liu Q, Yan J, Zhou F, Wang C. Electrochemical deposition of Au–Pt alloy particles with cauliflower-like microstructures for electro catalytic methanol oxidation. Int. J. Hydrogen Energy. 2012;37:4088-4097.

9. Antolini E. Carbon supports for low-temperature fuel cell catalysts. Appl. Catal. B Environ. 2009;88:1-24.

10. Steigerwalt ES, Deluga GA, Cliffel DE, Lukehart CM. A Pt−Ru/graphitic carbon nano fiber nano composite exhibiting high relative performance as a direct-methanol fuel cell anode catalyst. J. Phys. Chem. B. 2001;105:8097-8101.

11. Li W, Liang C, Zhou W, Qiu J, Zhenhua, Sun G, Xin Q. Preparation and characterization of multi walled carbon nano tube-supported platinum for cathode catalysts of direct methanol fuel cells. J. Phys. Chem. B. 2003;107:6292-6299.

12. Cheon JY, Ahn C, You DJ, Pak C, Hur SH, Kim J, Joo SH. Ordered meso-porous carbon–carbon nanotube nano composites as highly conductive and durable cathode catalyst supports for polymer electrolyte fuel cells. J. Mater. Chem. A. 2013;1: 1270-1283.

13. Coulon E, Pinson J, Bourzat JD, Commercon A, Pulicani JP. Electrochemical attachment of organic groups to carbon felt surfaces. Langmuir. 2001;17:7102-7106.

14. Zhu Y, Murali S, Cai W, Li X, Suk JW, Potts JR, Ruoff RS. Graphene and graphene oxide: Synthesis, Properties, and Applications. Adv. Mater. 2010; 22:3906-3924.

15. Geim AK, Novoselov KS. The rise of graphene. Nat. Mater. 2007;6:183-191.

16. Li JH, Li YM, Tang LH. Preparation and electrochemical performance for methanol oxidation of pt/graphene nano composites. Electrochem. Commun. 2009;11:846-849.

17. Yin GP, Zhang S, Shao YY, Liao HJ, Engelhard MH, Lin YH. Polyelectrolyte-induced reduction of exfoliated graphite oxide: a facile route to synthesis of soluble graphene nano sheets. ACS Nano. 2011; 5:1785-1791.

18. Wang EW, Guo SJ, Dong SJ. Three-dimensional Pt-on-Pd bimetallic nano dendrites supported on graphene nano sheet: facile synthesis and used as an advanced nano electro catalyst for methanol oxidation. ACS Nano. 2010; 4:547-555.

19. Guo S, Wen D, Zhai Y, Dong S, Wang E. Platinum nano particle ensemble-on-graphene hybrid nano sheet: One-pot, rapid synthesis, and used as new electrode material for electrochemical sensing. ACS Nano. 2010;4:3959-3968.

20. Kundu P, Nethravathi C, Deshpande PA, Rajamathi M, Madras G, Ravishankar N. Ultrafast microwave-assisted route to surfactant-free ultrafine Pt nanoparticles on graphene: Synergistic co-reduction mechanism and high catalytic activity. Chem. Mater. 2011;23:2772-2780.

21. Sharma S, Ganguly A, Papakonstantinou P, Miao X, Li M, Hutchison JL, Delichatsios M, Ukleja S. Rapid microwave synthesis of CO tolerant reduced graphene oxide-supported platinum electro catalysts for oxidation of methanol. J. Phys. Chem. C. 2010;114:19459-19466.

22. Chen X, Su B, Wu G, Yang CJ, Zhuang Z, Wang X, Chen X. Platinum nano flowers supported on graphene oxide nano sheets: their green synthesis, growth mechanism, and advanced electro catalytic properties for methanol oxidation. J. Mater. Chem. 2012;22:11284-11289.

23. Divya P, Ramaprabhu S. Platinum–graphene hybrid nanostructure as anode and cathode electro catalysts in proton exchange membrane fuel cells. J. Mater. Chem. A. 2014;2:4912-4918.

24. Tung VC, Chen LM, Allen MJ, Wassei JK, Nelson K, Kaner RB, Yang Y. Low-temperature solution processing of graphene−carbon nano tube hybrid materials for high-performance transparent conductors. Nano Lett. 2009;9:1949-1955.

25. Shao Y, Wang J, Engelhard M, Wang C, Lin Y. Facile and controllable electrochemical reduction of graphene oxid e and its applications. J. Mater. Chem. 2010;20:743-748.

26. Chen L, Tang Y, Wang K, Liu C, Luo S. Direct electro deposition of reduced graphene oxide on glassy carbon electrode and its electrochemical application. Electrochemistry Communications. 2011; 13:133-137.

27. Eda G, Fanchini G, Chhowalla M. Large-area ultrathin films of reduced graphene oxide as a transparent and flexible electronic material. Nature Nanotechnol. 2008;3:270-274.

27b. Kung C, Lin P, Xue Y, Akolkar R, Dai L, Yu X, Liu C. Three dimensional graphene foam supported platinum–ruthenium bimetallic nanocatalysts for direct methanol and direct ethanol fuel cell applications, Journal of Power Sources; 2014. DOI: 10.1016/ j.jpowsour.2014.01.074.

28. Hummers WS, Ofmann RE. Preparation of graphitic oxide. J. Am. Chem. Soc. 1958;80:1339-1339.

29. Das D, Ghosh S, Basumallick I. Electrochemical studies on glucose oxidation in an enzymatic fuel cell with enzyme immobilized on to reduced graphene oxide surface. Electroanalysis. 2014;26:2408-2418.

30. Choi EY, Han TH, Hong J, Kim JE, Lee SH, Kim HW, Kim SO. Noncovalent functionalization of graphene with end-functional polymers. J Mater. Chem. 2010; 20:1907-1912.

31. Dreyer DR, Park S, Bielawski CW, Ruoff RS. The chemistry of graphene oxide. Chem. Soc. Rev. 2010;39:228-240.

32. He D, Cheng K, Li H, Peng T, Xu F, Mu S, Pan M. Highly active platinum nanoparticles on graphene nano sheets with a significant improvement in stability and CO tolerance. Langmuir. 2012; 28:3979-3986.

33. Clare GL, Kucernak A. Determination of the platinum and ruthenium surface areas in platinum−ruthenium alloy electro catalysts by under potential deposition of copper. i. unsupported catalysts. J Phys. Chem. B 2002;106:1036-1047.

34. Tapan NA. A Mechanistic Approach to Elucidate Ethanol Electro-oxidation. Turk J. Chem. 2007;31:427-443.

35. Hitmi H, Belgsir EM, Leger JM, Lamy C, Lenza RO. A kinetic analysis of the electro-oxidation of ethanol at a platinum electrode in acid medium. Electrochim Acta. 1994;39:407-415.

36. Rodriguez P, Kwon Y, Koper M. The promoting effect of adsorbed carbon monoxide on the oxidation of alcohols on a gold catalyst. Nature Chem. 2012;4:177-182.

Peer-review history:
The peer review history for this paper can be accessed here:
http://www.sciencedomain.org/review-history.php?iid=775&id=5&aid=8517